

# Distinctive signals of boosted dark matter from semi-annihilations

Takashi Toma<sup>1,2\*</sup>

<sup>1</sup>*Institute of Liberal Arts and Science, Kanazawa University, Kanazawa, 920-1192 Japan*

<sup>2</sup>*Institute for Theoretical Physics, Kanazawa University, Kanazawa 920-1192, Japan*

## Abstract

Boosted dark matter can be produced by some mechanism and detecting it is a key to understand the nature of dark matter. We show that the semi-annihilation  $\chi\chi \rightarrow \bar{\chi}\nu$  indicates signals distinctive from the other semi-annihilation and standard dark matter annihilation processes. Since the boosted dark matter produced by this semi-annihilation is regarded as a high energy neutrino, the total flux of the dark matter and the accompanying neutrino yields double peaks at the energy close to the dark matter mass. Both of the particles can be detectable at large volume neutrino detectors.

---

\*toma@staff.kanazawa-u.ac.jp

# 1 Introduction

Nature of dark matter in the universe is still unknown, and its exploration is a primary subject of astro-particle physics. Weakly Interacting Massive Particles (WIMPs) are one of the well-motivated dark matter candidates. The WIMP particles are thermally produced in the early universe by sufficient interactions with the Standard Model (SM) particles, and the relic abundance is determined by so-called freeze-out mechanism without dependence of initial conditions. However no clear evidence is found so far, and strong constraints are imposed for WIMPs. In particular, the current constraints of the direct detection experiments are considerably severe. The XENON1T and PandaX-4T Collaborations have set an upper bound on WIMP-nucleon spin-independent (SI) elastic scattering cross section of  $4.1 \times 10^{-47} \text{ cm}^2$  and  $3.3 \times 10^{-47} \text{ cm}^2$  at a WIMP mass of 30 GeV, respectively [1, 2]. One of the ideas accommodating these strong constraints is to consider velocity-suppressed cross sections such as a pseudo-Nambu-Goldstone boson dark matter [3], or a fermion dark matter with a pseudo-scalar mediator [4].

On the other hand, semi-annihilating dark matter is a kind of WIMPs which emerges if the dark sector is non-minimally extended. In general, semi-annihilations are the process  $\chi\chi \rightarrow \bar{\chi}X$  with a (anti-)dark matter particle  $\chi(\bar{\chi})$  and a SM particle  $X$  in the final state.<sup>1</sup> This kind of dark matter is also thermally produced via freeze-out mechanism like WIMPs while it has relatively weaker interactions with the SM particles compared to WIMPs. For example, when an extra  $U(1)$  symmetry is spontaneously broken to a  $\mathbb{Z}_3$  symmetry, the lightest  $\mathbb{Z}_3$  charged particle can be a candidate of semi-annihilating dark matter. Semi-annihilations possess some interesting features different from standard annihilations. First, the semi-annihilating dark matter cannot be a self-conjugate particle in minimal models because of the charge conservation for the semi-annihilating processes as can be seen from  $\chi\chi \rightarrow \bar{\chi}X$ . Second, semi-annihilations produce relativistic (anti-)dark matter particles. This boosted dark matter may be detectable through large volume neutrino detectors such as Super-Kamiokande (SK) [5] and IceCube/DeepCore and its next generation experiments Hyper-Kamiokande (HK) [6] and PINGU [7], or Deep Underground Neutrino Experiment (DUNE) [8] and KN3NeT [9]. Therefore these can be distinctive features of semi-annihilating dark matter.

In this paper, we consider one of the most native semi-annihilation process  $\chi\chi \rightarrow \bar{\chi}\nu$  where  $\nu$  is the light neutrino in the SM, and investigate the simultaneous detection of both particles in the final state at large volume neutrino detectors such as SK/HK [6] and DUNE [8]. The similar signals of boosted dark matter from the Galactic center and the Sun have been explored in refs. [10–12]. Furthermore, the boosted dark matter signals induced from excited dark matter and multi-component dark matter scenarios have also been studied [13–15]. However the semi-annihilation process we focus on in this paper

---

<sup>1</sup>The corresponding CP conjugate process  $\bar{\chi}\bar{\chi} \rightarrow \chi\bar{X}$  also exists.

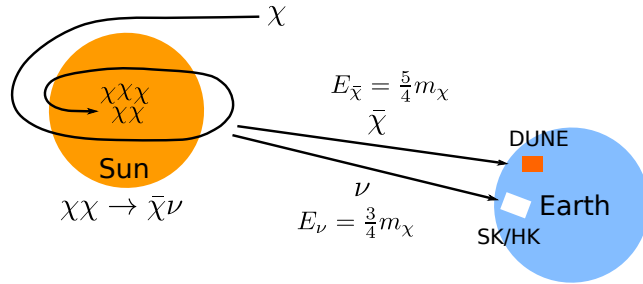


Figure 1: Schematic picture of the neutrino and boosted dark matter signals produced by the dark matter semi-annihilation at the Sun. Both particles can be detectable at large volume neutrino detectors SK/HK and DUNE.

provide simultaneous signals of a high energy neutrino and a boosted dark matter which are closely correlated with each other. This is different from the previous works, and become a distinctive feature of the semi-annihilation process. The schematic picture is depicted in Fig. 1.

## 2 Flux from the Sun

We focus on the neutrino and boosted dark matter flux originated from the semi-annihilation process  $\chi\chi \rightarrow \bar{\chi}\nu$  in the Sun. Although one can also consider the flux from the Galactic center or dwarf spheroidal galaxies, the resultant flux of  $\bar{\chi}$  and  $\nu$  are smaller than those from the Sun [10, 11]. The energy spectra of the neutrino and anti-dark matter flux from the Sun are given by [16, 17]

$$\frac{d\Phi_{\nu/\bar{\chi}}}{dE_{\nu/\bar{\chi}}} = \frac{\Gamma_{\text{ann}}}{4\pi d_{\odot}^2} \frac{dN_{\nu/\bar{\chi}}}{dE_{\nu/\bar{\chi}}}, \quad (2.1)$$

where  $d_{\odot} = 1.5 \times 10^{13}$  cm is the distance between the Sun and the Earth,  $dN_{\nu/\bar{\chi}}/dE_{\nu/\bar{\chi}}$  is the energy spectra of  $\nu$  and  $\bar{\chi}$ , and  $\Gamma_{\text{ann}}$  is the annihilation rate which is proportional to the semi-annihilation cross section times the squared number of accumulated dark matter particles in the Sun:  $\langle \sigma_{\chi\chi \rightarrow \bar{\chi}\nu} \rangle N_{\chi}^2$ . The energy of  $\nu$  and  $\bar{\chi}$  are fixed at  $E_{\nu} = 3m_{\chi}/4$  and  $E_{\bar{\chi}} = 5m_{\chi}/4$  for  $\chi\chi \rightarrow \bar{\chi}\nu$  since the annihilating dark matter particles are non-relativistic. Thus the energy spectra  $dN_{\nu/\bar{\chi}}/dE_{\nu/\bar{\chi}}$  are simply given by the delta functions, and the energy difference between  $\nu$  and  $\bar{\chi}$  is exactly fixed to be  $E_{\bar{\chi}} - E_{\nu} = m_{\chi}/2$ . The total combined flux would exhibit double peak structure which is a novel discriminative feature of this semi-annihilation process. Note that it is implicitly assumed above that all the observed relic abundance is occupied by the dark matter  $\chi$  for simplicity, namely asymmetric dark matter. However this is not essential assumption for the signals, and the CP conjugate process  $\bar{\chi}\bar{\chi} \rightarrow \chi\bar{\nu}$  should also be taken into account if both of  $\chi$  and  $\bar{\chi}$  exist.

The dark matter particles are captured in the center of the Sun due to the energy loss via the elastic scattering with nucleons while the number of the accumulated anti-dark matter particles decrease via the semi-annihilation. Here we assume the spin-dependent (SD) elastic scattering cross section  $\sigma_{\text{SD}}$  is dominant over the SI cross section and it is velocity dependent ( $\sigma_{\text{SD}} \propto v^2$  with the dark matter velocity  $v$ ) since the SI cross section is strongly constrained by the dark matter direct detection experiments [1,2]. This velocity dependence leads significant enhancement of the boosted dark matter signals at the detectors since the typical dark matter local velocity is  $v \sim 10^{-3}$  while it is  $v = 0.6$  for the boosted dark matter.

Evaporation effects of the accumulated dark matter particles in the Sun can be negligible if the dark matter mass is heavier than a few GeV [18]. Then, equilibrium between the capture and the semi-annihilation process is reached after enough time, and the number of the dark matter particles in the Sun becomes a constant. In this case, the annihilation rate in Eq. (2.1) can be written in terms of the capture rate which is proportional to  $\sigma_{\text{SD}}$  as [11]

$$\Gamma_{\text{ann}} \approx 2.6 \times 10^{21} [\text{s}^{-1}] \left( \frac{1 \text{ TeV}}{m_\chi} \right)^2 \left( \frac{\sigma_{\text{SD}}}{10^{-40} \text{ cm}^2} \right). \quad (2.2)$$

Note that the rate has an enhancement of about factor 20 compared to a constant  $\sigma_{\text{SD}}$  [11].

Although the SD elastic scattering cross section is also constrained by the direct detection experiments, it is not as strong as the SI cross section [19,20]. In fact, the PICO-60 experiment has set the strongest bound for  $m_\chi \lesssim 100 \text{ GeV}$  using 52kg of  $\text{C}_3\text{F}_8$  [21], which is given by  $3.4 \times 10^{-41} \text{ cm}^2$  for a 30 GeV WIMP mass. For a heavier dark matter mass, the strongest upper bound comes from the neutrino observation at IceCube [22]. The bound depends on dark matter annihilation channels, and is especially strong for  $\tau\bar{\tau}$  and  $\nu\bar{\nu}$  channels. We adopt the  $\nu\bar{\nu}$  bound in ref. [22] with a factor 1/2 taking into account the fact that only one neutrino is produced at the semi-annihilation. This is translated into an upper bound on the annihilation rate  $\Gamma_{\text{ann}}$ . Therefore this implies that the flux of the neutrino and the boosted dark matter is also bounded from above as

$$\Phi_{\nu/\bar{\chi}} \leq 5.2 \times 10^{-9} [\text{cm}^{-2}\text{s}^{-1}] \left( \frac{1 \text{ TeV}}{m_\chi} \right)^2 \left( \frac{\sigma_{\text{SD}}^{\text{exp}}}{10^{-41} \text{ cm}^2} \right), \quad (2.3)$$

where  $\sigma_{\text{SD}}^{\text{exp}}$  is the experimental upper bound of the SD cross section.

An example of the combined flux of  $\nu$  and  $\bar{\chi}$  is shown in Fig. 2 where the delta functions have been filtered with a Gaussian kernel taking into account a detector energy resolution [23]. The total flux indicates double peak structure at  $E_\nu$  and  $E_{\bar{\chi}}$ . The atmospheric neutrinos can be the primary background for the signals, and thus the total atmospheric muon neutrino flux observed at SK and IceCube are also shown. Although the atmospheric electron neutrinos also exists, the  $\nu_e$  flux is much smaller for the energy larger than  $\mathcal{O}(10) \text{ GeV}$ .

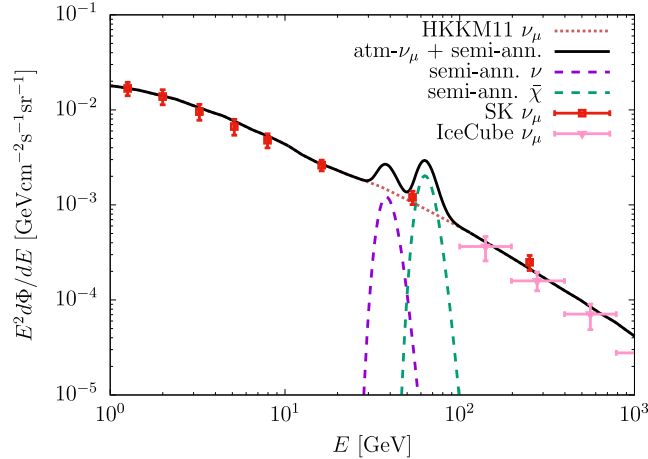


Figure 2: Double peak structure of the signal flux from the Sun where the energy resolution of  $\Delta E/E = 25\%$  is assumed for the energy spectra. The dark matter mass and the SD elastic scattering cross section are chosen as  $m_\chi = 50$  GeV and  $\sigma_{\text{SD}} = 3 \times 10^{-41}$  cm<sup>2</sup>. The red and pink points represent the experimental data of SK and IceCube, respectively [24]. The dark pink dotted line is the fitting with the HKKM11 model [25].

### 3 Boosted dark matter signal at DUNE

DUNE consists of two detectors located at the Fermi National Accelerator Laboratory and the Sanford Underground Research Laboratory [8]. The latter one installs 40kton fiducial mass of liquid argon and can search for the signal of the boosted dark matter using Liquid Argon Time Projection Chamber (LArTPC) due to the scattering off a proton in the LArTPC.<sup>2</sup>

The expected signal events of the boosted dark matter can be estimated by

$$N_{\text{sig}} = t_{\text{exp}} \cdot N_p \cdot \Phi_{\bar{\chi}} \cdot \tilde{\sigma}_{\text{SD}} \cdot \epsilon_{\text{eff}}, \quad (3.1)$$

where  $t_{\text{exp}}$  is the exposure time,  $N_p$  is the number of the target protons at the detector,  $\Phi_{\bar{\chi}}$  is the flux from the Sun,  $\tilde{\sigma}_{\text{SD}}$  is the scattering cross section of the boosted dark matter with a proton in argon and  $\epsilon_{\text{eff}}$  is the detector efficiency.

The elastic scattering cross section for the boosted dark matter ( $\tilde{\sigma}_{\text{SD}}$ ) is different from  $\sigma_{\text{SD}}$  which has been appeared in the flux calculation above. Since the SD cross section is assumed to be velocity-suppressed ( $\sigma_{\text{SD}} \propto v^2$ ), the cross section for the boosted dark matter  $\tilde{\sigma}_{\text{SD}}$  is approximately estimated as  $\tilde{\sigma}_{\text{SD}} \sim 3.6 \times 10^5 \sigma_{\text{SD}}$  taking into account the velocity difference between the non-relativistic and boosted dark matter particles. Note that the effect of the nucleon form factors should also be taken into account which is expected to induce  $\mathcal{O}(1)$  difference [10, 11, 26].

<sup>2</sup>Although scattering off a neutron can also be a signal, this event reconstruction is relatively harder than protons.

From the kinematics of the elastic scattering, the energy of the scattered proton  $E_p$  is determined in the range of

$$m_p \leq E_p \leq m_p \frac{(E_{\bar{\chi}} + m_p)^2 + E_{\bar{\chi}}^2 - m_{\chi}^2}{(E_{\bar{\chi}} + m_p)^2 - E_{\bar{\chi}}^2 + m_{\chi}^2}, \quad (3.2)$$

in the rest frame of the proton [10]. Since the energy of the boosted dark matter is fixed to be  $E_{\bar{\chi}} = 5m_{\chi}/4$ , the energy of the scattered proton is determined as

$$m_p \leq E_p \lesssim \frac{17}{8}m_p, \quad (3.3)$$

where  $m_p \ll m_{\chi}$  is assumed. Thus the proton energy is less 2 GeV and independent of the dark matter mass. In this energy range, resonant scatterings and deep inelastic scatterings can be ignored [26]. This energy is not enough to emit a Cherenkov light in water and ice at such as SK/HK and IceCube. However it is anticipated to be observed at DUNE since the thresholds of the proton kinetic energy and angular resolution are as low as 50 MeV and  $5^\circ$ , respectively [27]. These precise measurement significantly reduces the main background events of the atmospheric neutrinos [10].

The detector efficiency  $\epsilon_{\text{eff}}$  is estimated in the range of  $0.80 \lesssim \epsilon_{\text{eff}} \lesssim 0.95$  for electron neutrinos and muon neutrinos via the charged current interaction when the neutrino energy is in the range of 1 GeV to 2 GeV [27]. Since there is no estimation of  $\epsilon_{\text{eff}}$  for the boosted dark matter, we choose  $\epsilon_{\text{eff}} = 0.80$  as a benchmark.

The expected number of the signal events per a year at DUNE is shown in Fig. 3. The number of the target protons with the 40 kton fiducial mass of liquid argon is  $N_p = 1.1 \times 10^{34}$ . The upper gray region is excluded by the bound of the SD cross section in non-relativistic limit. The red triangle is a sample parameter point which has been adopted for Fig. 2. For a realistic detection of the boosted dark matter signal, a benchmark of the number of events is set to be 10 events per a year, which is shown as the green dotted line in Fig. 3. From the figure, one can see that the dark matter mass should be  $m_{\chi} \lesssim \mathcal{O}(100)$  GeV so that the required number of events occur. The expected number of the signal events at the sample parameter point (red triangle) is 18 per a year. The above calculation is no more than rough estimation, and more detailed simulation at DUNE can be done following the ref. [8, 26]. Although we have not taken into account the effect of the neutrino flavor change via neutrino oscillations, it should be included for more sophisticated analysis.

The accompanying neutrino may also induce another signal  $\nu p \rightarrow \nu p$  at different energy scale. Since  $E_{\nu} \gg m_p$ , the deep inelastic scattering dominates in this case. The energy range of the scattered proton is given by  $m_p \leq E_p \lesssim m_{\chi}$  from Eq. (3.2). If the DUNE experiment allows the neutrino signal search in this energy range, both characteristic signals of the boosted dark matter and the neutrinos from the semi-annihilation process can be searched simultaneously at DUNE, which is the best scenario. Even if this

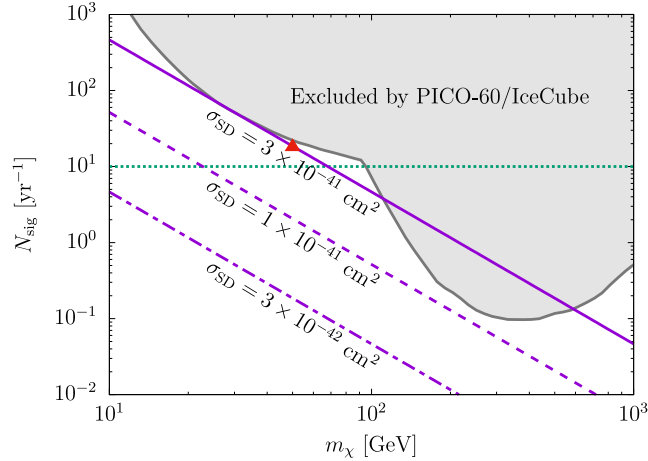


Figure 3: Expected number of the signal events at DUNE where the detector efficiency is taken as  $\epsilon_{\text{eff}} = 0.80$ . The red triangle is a sample parameter point used for Fig. 2. The upper gray region is excluded by PICO-60 [21] and IceCube [22].

is not the case because of too large neutrino energy (corresponding to heavy dark matter mass), the signals from the accompanying neutrinos can be searched at SK/HK.

## 4 Model building

A velocity-dependent SD cross section is assumed in the above argument. Such a cross section can be derived from anapole moment or scalar-pseudoscalar (SP) interaction given by [28]

$$\mathcal{L}_{\text{ana}} = \frac{1}{\Lambda^2} \bar{\chi} \gamma_\mu \gamma_5 \partial_\nu \chi F^{\mu\nu}, \quad (4.1)$$

$$\mathcal{L}_{\text{SP}} = \frac{1}{\Lambda^2} (\bar{\chi} \chi) (\bar{q} \gamma_5 q), \quad (4.2)$$

where  $\Lambda$  is a cut-off scale of the theory, and  $F^{\mu\nu}$  is the electromagnetic field strength which is contracted to the electromagnetic current  $eA_\mu J^\mu$  in order to induce an elastic scattering with a proton. The resultant SD cross sections from the above interactions are suppressed by velocity-squared ( $\sigma_{\text{SD}} \propto v^2$ ). However note that for the anapole moment interaction a SI cross section with the  $v^2$  suppression also emerges at the same time.

In addition, the pseudoscalar-pseudoscalar (PP) interaction

$$\mathcal{L}_{\text{PP}} = \frac{1}{\Lambda^2} (\bar{\chi} \gamma_5 \chi) (\bar{q} \gamma_5 q), \quad (4.3)$$

induces further suppressed SD cross section ( $\sigma_{\text{SD}} \propto v^4$ ). In this case, the standard annihilation cross section for  $\chi \bar{\chi} \rightarrow q \bar{q}$  induced from the above PP interaction by crossing

symmetry corresponds to  $s$ -wave, and the model is strongly constrained by gamma ray observations of the MAGIC and Fermi-LAT Collaborations if the dark matter mass is below  $\mathcal{O}(100)$  GeV [29].

When the velocity-suppression is extremely strong like the above PP interaction, one should also be careful with loop corrections once a ultra-violet (UV) complete model is built. The loop corrections may induce a new contribution to the cross section which is not velocity-suppressed, and becomes dominant over the velocity-suppressed cross sections depending on the parameters.

In the UV complete models with radiative neutrino masses [30,31], and its further extensions [32], the semi-annihilation process  $\chi\chi \rightarrow \bar{\chi}\nu$  can naturally occur. In these models, although neutrino masses at the tree level are forbidden by the imposed  $\mathbb{Z}_3$  symmetry, the small masses are induced at the two-loop level. This symmetry also stabilizes the lightest  $\mathbb{Z}_3$  charged fermion and provides a dark matter candidate with the semi-annihilation process.

## 5 Summary and discussions

We have found a novel signals of the neutrino and the boosted dark matter from the semi-annihilation  $\chi\chi \rightarrow \bar{\chi}\nu$  induced from the Sun. These two signals are correlated with each other and can be distinctive from the other semi-annihilation and standard dark matter annihilation processes. We have approximately estimated the neutrino and the boosted dark matter flux from the Sun assuming a velocity-suppressed SD cross section. Both of the produced neutrino and boosted dark matter can be detected at DUNE and SK/HK. We have also performed the simple estimation for the number of the signal events at DUNE, and found that the dark matter mass should be  $m_\chi \lesssim \mathcal{O}(100)$  GeV so that a realistic number of the signal events are produced. If the signals of the semi-annihilation are experimentally confirmed, it strongly suggests that the dark matter is a Dirac fermion with spin 1/2.

Our framework can be applied to the other boosted dark matter scenarios like models with multi-component dark matter. In this case, the correlation between the two signals would be weaker since the heavier dark matter captured in the Sun and the lighter boosted dark matter which can be detectable at DUNE are different particles. Furthermore, the similar argument with a velocity-dependent SI cross section can also be studied. In this case, the expected  $\nu$  and  $\bar{\chi}$  fluxes are smaller than the case we considered, and thus heavier dark matter mass range would be a target of signal search to be consistent with the background atmospheric neutrinos. This scenario may provide an implication for the future neutrino experiments PINGU and KM3NeT.



# Acknowledgments

The author would like to thank Mayumi Aoki for careful reading of the manuscript and valuable comments. This work was supported by JSPS Grant-in-Aid for Scientific Research KAKENHI Grant No. JP20K22349. Numerical computation in this work was carried out at the Yukawa Institute Computer Facility.

# References

- [1] E. Aprile *et al.* [XENON], Phys. Rev. Lett. **121**, no.11, 111302 (2018) [[arXiv:1805.12562](#) [astro-ph.CO]].
- [2] Y. Meng *et al.* [PandaX-4T ], [[arXiv:2107.13438](#) [hep-ex]].
- [3] C. Gross, O. Lebedev and T. Toma, Phys. Rev. Lett. **119**, no.19, 191801 (2017) [[arXiv:1708.02253](#) [hep-ph]].
- [4] S. Ipek, D. McKeen and A. E. Nelson, Phys. Rev. D **90**, no.5, 055021 (2014) [[arXiv:1404.3716](#) [hep-ph]].
- [5] C. Kachulis *et al.* [Super-Kamiokande], Phys. Rev. Lett. **120**, no.22, 221301 (2018) [[arXiv:1711.05278](#) [hep-ex]].
- [6] K. Abe *et al.* [Hyper-Kamiokande], [[arXiv:1805.04163](#) [physics.ins-det]].
- [7] M. G. Aartsen *et al.* [IceCube-PINGU], [[arXiv:1401.2046](#) [physics.ins-det]].
- [8] B. Abi *et al.* [DUNE], [[arXiv:2002.03005](#) [hep-ex]].
- [9] S. Adrian-Martinez *et al.* [KM3Net], J. Phys. G **43**, no.8, 084001 (2016) [[arXiv:1601.07459](#) [astro-ph.IM]].
- [10] K. Agashe, Y. Cui, L. Necib and J. Thaler, JCAP **10**, 062 (2014) [[arXiv:1405.7370](#) [hep-ph]].
- [11] J. Berger, Y. Cui and Y. Zhao, JCAP **02**, 005 (2015) [[arXiv:1410.2246](#) [hep-ph]].
- [12] D. McKeen and N. Raj, Phys. Rev. D **99**, no.10, 103003 (2019) [[arXiv:1812.05102](#) [hep-ph]].
- [13] D. Kim, J. C. Park and S. Shin, Phys. Rev. Lett. **119**, no.16, 161801 (2017) [[arXiv:1612.06867](#) [hep-ph]].
- [14] M. Aoki and T. Toma, JCAP **10**, 020 (2018) [[arXiv:1806.09154](#) [hep-ph]].
- [15] D. Kim, J. C. Park and S. Shin, Phys. Rev. D **100**, no.3, 035033 (2019) [[arXiv:1903.05087](#) [hep-ph]].
- [16] G. Belanger, F. Boudjema, A. Pukhov and A. Semenov, Comput. Phys. Commun. **185**, 960-985 (2014) [[arXiv:1305.0237](#) [hep-ph]].

- [17] P. Baratella, M. Cirelli, A. Hektor, J. Pata, M. Piibeleht and A. Strumia, JCAP **03**, 053 (2014) [[arXiv:1312.6408](#) [hep-ph]].
- [18] G. Busoni, A. De Simone and W. C. Huang, JCAP **07**, 010 (2013) [[arXiv:1305.1817](#) [hep-ph]].
- [19] E. Aprile *et al.* [XENON], Phys. Rev. Lett. **122**, no.14, 141301 (2019) [[arXiv:1902.03234](#) [astro-ph.CO]].
- [20] J. Xia *et al.* [PandaX-II], Phys. Lett. B **792**, 193-198 (2019) [[arXiv:1807.01936](#) [hep-ex]].
- [21] C. Amole *et al.* [PICO], Phys. Rev. Lett. **118**, no.25, 251301 (2017) [[arXiv:1702.07666](#) [astro-ph.CO]].
- [22] M. G. Aartsen *et al.* [IceCube], JCAP **04**, 022 (2016) [[arXiv:1601.00653](#) [hep-ph]].
- [23] G. Bertone, C. B. Jackson, G. Shaughnessy, T. M. P. Tait and A. Vallinotto, Phys. Rev. D **80**, 023512 (2009) [[arXiv:0904.1442](#) [astro-ph.HE]].
- [24] E. Richard *et al.* [Super-Kamiokande], Phys. Rev. D **94**, no.5, 052001 (2016) [[arXiv:1510.08127](#) [hep-ex]].
- [25] M. Honda, T. Kajita, K. Kasahara and S. Midorikawa, Phys. Rev. D **83**, 123001 (2011) [[arXiv:1102.2688](#) [astro-ph.HE]].
- [26] J. Berger, Y. Cui, M. Graham, L. Necib, G. Petrillo, D. Stocks, Y. T. Tsai and Y. Zhao, Phys. Rev. D **103**, no.9, 095012 (2021) [[arXiv:1912.05558](#) [hep-ph]].
- [27] R. Acciarri *et al.* [DUNE], [[arXiv:1512.06148](#) [physics.ins-det]].
- [28] G. B. Gelmini, V. Takhistov and S. J. Witte, JCAP **07**, 009 (2018) [erratum: JCAP **02**, E02 (2019)] [[arXiv:1804.01638](#) [hep-ph]].
- [29] M. L. Ahnen *et al.* [MAGIC and Fermi-LAT], JCAP **02**, 039 (2016) [[arXiv:1601.06590](#) [astro-ph.HE]].
- [30] E. Ma, Phys. Lett. B **662**, 49-52 (2008) [[arXiv:0708.3371](#) [hep-ph]].
- [31] M. Aoki and T. Toma, JCAP **09**, 016 (2014) [[arXiv:1405.5870](#) [hep-ph]].
- [32] S. Y. Ho, T. Toma and K. Tsumura, Phys. Rev. D **94**, no.3, 033007 (2016) [[arXiv:1604.07894](#) [hep-ph]].